

Crystal structure and physical properties of $\text{Eu}_{0.83}\text{Fe}_4\text{Sb}_{12}$

E. Bauer, St. Berger, A. Galatanu,* M. Galli,† H. Michor, G. Hilscher, and Ch. Paul
Institut für Experimentalphysik, Technische Universität Wien, Wiedner Hauptstraße 8-10, A-1040 Wien, Austria

B. Ni and M. M. Abd-Elmeguid
Physikalisches Institut, Universität Köln, Zùlpicher Strasse 77, D-50937 Köln, Germany

V. H. Tran,‡ A. Grytsiv, and P. Rogl
Institut für Physikalische Chemie, Universität Wien, Währingerstrae 42, A-1090 Wien, Austria
 (Received 9 November 2000; revised manuscript received 18 January 2001; published 22 May 2001)

$\text{Eu}_{0.83}\text{Fe}_4\text{Sb}_{12}$, was synthesized by arc melting in homogeneous practically single phase form. From Rietveld refinement isotypism was derived with the $\text{LaFe}_4\text{P}_{12}$ -(skutterudite)-type, space group $Im\bar{3}$, No. 204. The refinement also served to determine the Eu content of $x=0.83(2)$. $\text{Eu}_{0.83}\text{Fe}_4\text{Sb}_{12}$ orders magnetically below 84 K and isothermal magnetization measurements reveal a spontaneous magnetization reaching about $4.5\mu_B/\text{f.u.}$ at 6 T. The electronic configuration of the Eu ion in this compound appears to be close to the $4f^7$ state, thus behaving almost divalently. From the measurements of transport coefficients, the figure of merit Z was evaluated as $ZT \approx 0.08$ at room temperature. The most outstanding property of this compound, however, is the significant magnetoresistance of about 130% at $T=1$ K for a magnetic field of 12 T but still 30% near room temperature.

DOI: 10.1103/PhysRevB.63.224414

PACS number(s): 72.15.Eb, 72.15.Jf, 76.80.+y, 84.60.Bk

I. INTRODUCTION

Skutterudites TM_3 with $T=\text{Co, Ni, Rh, and Ir}$ and $M=\text{P, As, and Sb}$ filled with electropositive elements have attracted much attention because of an unusually large figure of merit $Z=S^2/(\rho\lambda)$ being a basic requirement for thermoelectric applications (S , ρ , and λ are the Seebeck coefficient, the electrical resistivity, and the thermal conductivity, respectively).¹ Furthermore, these filled ternary compounds exhibit a rich variety of ground-state properties, whereby the magnetic behavior is dominated in particular by the $4f$ electronic configuration. Hence features like Kondo and heavy fermion behavior or various types of magnetic order, hopping conductivity, and superconductivity were already found.²⁻¹⁰

Ternary $\text{EuFe}_4\text{Sb}_{12}$ was reported to order ferromagnetically at $T=82$ K and the effective magnetic moment was found to be $8.4\mu_B$.⁶ The large magnitude of the effective moment indicates that the Eu ions do not exhibit the trivalent nonmagnetic state Eu^{3+} . If an effective moment of $2.6\mu_B$ is assumed for the Fe polyanions, the Eu moment is derived as $\mu_{\text{eff}} \approx 6.8\mu_B$,⁶ which has to be compared with the value of $\mu_{\text{eff}} \approx 7.94\mu_B$ for Eu^{2+} .

In this study, we present a survey of bulk properties of $\text{Eu}_{0.83}\text{Fe}_4\text{Sb}_{12}$ and isomorphous nonmagnetic $\text{La}_{0.83}\text{Fe}_4\text{Sb}_{12}$ and discuss the thermoelectric performance with respect to the figure of merit of that material.

II. EXPERIMENT

A. Synthesis

Starting materials were Eu ingots, pieces of iron, and rods of antimony (all 99.9 wt %). Due to the high vapor pressures of Eu and Sb at elevated temperatures, argon arc melting was

performed under minimal electric current with repeated melting whereby the alloy (about 4 g) was flipped over and every second time was fragmented into several pieces, the outer parts moved to inside positions prior to remelting. With this method and compensating for the losses of evaporation by additional Eu, a rather dense product was achieved. The alloy was then sealed under vacuum in silica capsules, slowly heated (50°C/h) to 700°C and kept there for 150 h followed by quenching in water. The pellets were found to be in a homogeneous state with only a minor amount of secondary phases such as free Sb, EuSb_2 , or Eu_2Sb_3 .

B. X-ray powder diffraction

X-ray powder-diffraction data were obtained using a Huber-Guinier powder camera applying monochromatic $\text{Cu K}\alpha_1$ radiation with an image plate recording system. Lattice parameters were calculated by least-squares fits to the indexed 4θ values applying the program package STRUKTUR (Ref. 11) on the base of our single-crystal data of $\text{YbFe}_4\text{Sb}_{12}$.¹² For quantitative refinement of the atom positions, x-ray intensities were recorded from a flat specimen from the Guinier image plate recordings. Full matrix-full profile Rietveld refinements employed the FULLPROF program.¹³

C. Measurements of bulk properties

The electrical resistivity and magnetoresistivity of bar-shaped samples were measured using a four-probe dc method in the temperature range from 0.4 K to room temperature and fields up to 12 T.

A liquid pressure cell with a 4:1 methanol-ethanol mixture as pressure transmitter served to generate hydrostatic

pressure up to about 15 kbar. The absolute value of the pressure was determined from the superconducting transition temperature of lead.¹⁴

Thermal-conductivity measurements were performed in a flow cryostat on cuboid-shaped samples (length: about 1 cm, cross section: about 2 mm²) that were kept cold by anchoring one end of the sample onto a thick copper panel mounted on the heat exchanger of the cryostat. The temperature difference along the sample, established by electrical heating, was determined by means of a differential thermocouple (Au + 0.07% Fe/chromel). The measurement was carried out under high vacuum and three shields mounted around the sample reduced the heat losses due to radiation at finite temperatures. The innermost of these shields was kept at the temperature of the sample via an extra heater maintained by a second temperature controller.

Thermopower measurements were carried out with a differential method. The absolute thermopower $S_x(T)$ was calculated using the following equation: $S_x(T) = S_{pb}(T) - V_{pb/x}/\Delta T$ where S_{pb} is the absolute thermopower of lead and $V_{pb/x}$ is the thermally induced voltage across the sample, depending on the temperature difference ΔT .

A superconducting quantum interference device magnetometer served to determine the magnetization from 2 up to 300 K in fields up to 6 T. Specific-heat measurements on samples of about 1–2 g were performed at temperatures ranging from 1.5 up to 120 K by means of a quasiadiabatic step heating technique.

¹⁵¹Eu Mössbauer-effect (ME) measurements were performed using a 100-mCi SmF₃ Mössbauer source at 300 and 4.2 K. Source and absorber were kept during the measurements at the same temperature in a He cryostat.

III. RESULTS AND DISCUSSION

A. Structural chemistry

The obtained x-ray intensity pattern was indexed on the base of a body-centered cubic lattice prompting isotypism with LaFe₄P₁₂.¹⁵ Some weak peaks could be identified as free antimony and were refined simultaneously with the main phase. The refinements of the x-ray intensities in all cases converged satisfactorily for a fully ordered atom arrangement Eu_yFe₄Sb₁₂ with respect to atom site distribution among Eu, Fe, and Sb atoms [$Im\bar{3}$; Sb in 24 g; $x_{Sb}=0$; $y_{Sb}=0.1609(1)$; $z_{Sb}=0.3383(1)$; $R_I=0.044$]. Occupation factors were refined and corresponded to a full occupancy of the Fe and Sb sublattice but revealed considerable voids for the Eu and La sites accounting for only 83% filling of the rare-earth site [$x=0.83(2)$]. The lattice parameter was found to be $a=9.1631(5)$ Å in the case of Eu_{0.83}Fe₄Sb₁₂ and $a=9.1486(4)$ Å in the case of La_{0.83}Fe₄Sb₁₂.

B. Bulk properties

1. Magnetic properties

Shown in Fig. 1 is the inverse magnetic susceptibility $\chi^{-1}(T)$ of Eu_{0.83}Fe₄Sb₁₂ as a function of temperature plotted for $\mu_0 H=1$ and 3 T. Above about 120 K, $\chi(T)$ can be

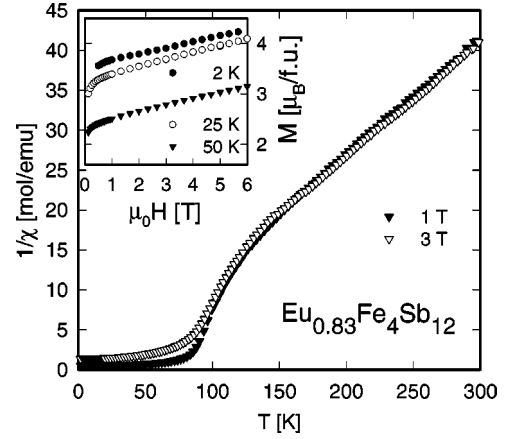


FIG. 1. Temperature-dependent inverse magnetic susceptibility $1/\chi$ of Eu_{0.83}Fe₄Sb₁₂ measured at $\mu_0 H=0.5$ T. The inset shows isothermal magnetization data of Eu_{0.83}Fe₄Sb₁₂.

described by a modified Curie-Weiss law $\chi(T) = \chi_0 + C/(T - \theta_p)$ with C the Curie constant, θ_p the paramagnetic Curie temperature, and a temperature-independent susceptibility contribution χ_0 . A least-squares fit yields an effective moment of $7.28\mu_B$ /f.u. and a paramagnetic Curie temperature of 19 K that indicates ferromagnetic interactions. In order to derive the effective magnetic moment of Eu, the magnetic state of the polyanion [Fe₄Sb₁₂] has to be taken into consideration. Measurements of, e.g., isomorphous LaFe₄Sb₁₂ and CaFe₄Sb₁₂ (Ref. 6) exhibit effective moments $\mu_{\text{eff}}=3.0$ and $3.7\mu_B$, respectively, which primarily have to be attributed to the magnetic behavior of Fe. As a consequence, the effective moment assigned to Eu is smaller than the measured one. Using the above results and assuming that both the rare-earth and the polyanion contribution to μ_{eff} is simply additive, i.e.,

$$\mu_{\text{eff}}^{\text{meas}} = \sqrt{0.83(\mu_{\text{eff}}^{\text{Eu}})^2 + (\mu_{\text{eff}}^{\text{polyan}})^2},$$

this yields $\mu_{\text{eff}}^{\text{Eu}}=7.28$ and $6.9\mu_B$ when comparing with LaFe₄Sb₁₂ and CaFe₄Sb₁₂, respectively. The former effective magnetic moment would coincide with a valency $\nu \approx 2.15$ of the Eu ion if a linear relationship is assumed for μ_{eff} between Eu²⁺ and Eu³⁺. It is interesting to note that the experimental value $\mu_{\text{eff}}=7.28\mu_B$ would also be compatible with an Eu²⁺ state and $y \approx 0.84$, a value slightly above the observed 83% occupation of the rare-earth site.

Well below 120 K, χ^{-1} vs T of Eu_{0.83}Fe₄Sb₁₂ strongly deviates from the Curie-Weiss behavior; the derived s -shaped curve is reminiscent of ferrimagnetic systems. Magnetic ordering occurs at $T_{\text{mag}} \approx 84$ K, in agreement with the work of Danebrock *et al.*⁶

In order to obtain more direct information on the valence state of Eu in Eu_{0.83}Fe₄Sb₁₂, we have performed ¹⁵¹Eu ME measurements on this sample at 300 and 4.2 K. The spectra collected at 300 and 4.2 K are displayed in Figs. 2(a) and (b). As evident from Fig. 2(a), the position of the ¹⁵¹Eu resonance line corresponds to a value of the isomer shift $IS = -11.69(6)$ mm/s, which clearly indicates that the valence state of Eu is nearly divalent. No resonance is observed, verifying the absence of a Eu³⁺ component in the sample. At

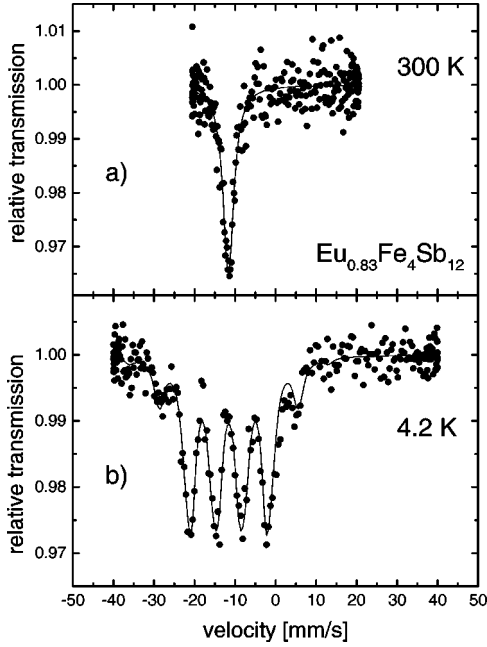


FIG. 2. ^{151}Eu Mössbauer spectra of $\text{Eu}_{0.83}\text{Fe}_4\text{Sb}_{12}$ collected at 300 (a) and 4.2 K (b). Solid lines through the data points are least-squares fits to the spectra.

low temperature (4.2 K) one observes a magnetic hyperfine split spectrum [hyperfine field, $B_{\text{eff}} = 23.8(2)$ T] due to the ordering of the Eu^{2+} ($^8S_{7/2}$) magnetic moments below T_{mag} [compare Fig. 2(b)]. The value of IS at 4.2 K remains almost unchanged [$IS = -11.52(5)$ mm/s] indicating a stable Eu^{2+} valence state. The slight decrease in IS is caused by the volume decrease due to the thermal expansion between 300 and 4.2 K.

Isothermal magnetization measurements on $\text{Eu}_{0.83}\text{Fe}_4\text{Sb}_{12}$ (see inset of Fig. 1) reveal a spontaneous magnetization of $3.55\mu_B$ for $T = 2$ K. With increasing fields, the magnetization rises, reaching $4.26\mu_B$ at 6 T. If all the Eu moments are aligned, the saturation magnetization should reach a value near that of Gd systems ($\vec{j} = \vec{s} = 7/2$, $\vec{l} = 0$), i.e., $\vec{M} = g\vec{j} = 7\mu_B$. The significantly smaller experimental values would then be consistent with ferrimagnetic order or some canted type of ferromagnetic coupling.

Magnetization measurements performed at $\mu_0 H = 0.02$ T evidence traces of an impurity phase that orders around 25 K. However, fields of the order of 0.1 T are sufficient to saturate this magnetic impurity contribution. Within the paramagnetic temperature region, the magnetization scales with the applied magnetic field.

2. Thermal properties

The temperature-dependent specific heat $C_p(T)$ of $\text{Eu}_{0.83}\text{Fe}_4\text{Sb}_{12}$ is plotted in Fig. 3 as C_p/T vs T . For the purpose of comparison, we have added the results of isostructural $\text{La}_{0.83}\text{Fe}_4\text{Sb}_{12}$, too. Magnetic ordering of $\text{Eu}_{0.83}\text{Fe}_4\text{Sb}_{12}$ around $T = 84$ K is derived from the distinct anomaly in $C_p(T)$. The impurity phase, as also observed from the magnetization measurement, causes a small

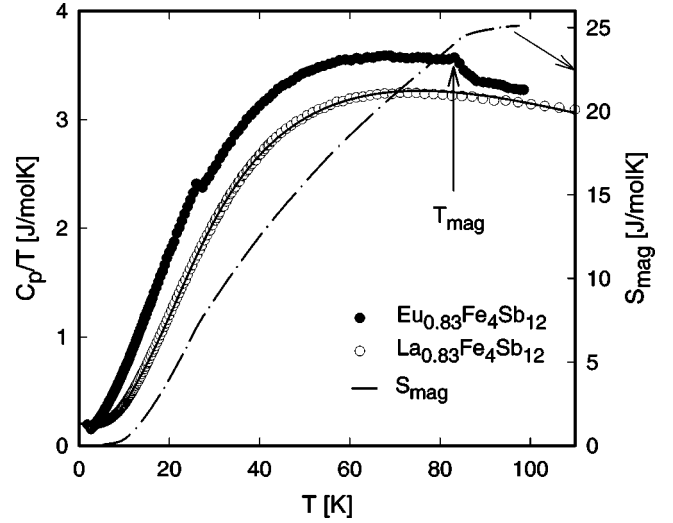


FIG. 3. Temperature-dependent specific heat C_p of $\text{Eu}_{0.83}\text{Fe}_4\text{Sb}_{12}$. For the purpose of comparison, C_p of $\text{La}_{0.83}\text{Fe}_4\text{Sb}_{12}$ is added. The solid line represents a least-squares fit according to Eq. (1) and the dashed line is the magnetic entropy S_{mag} of $\text{Eu}_{0.83}\text{Fe}_4\text{Sb}_{12}$.

anomaly at 25 K. While $C_p/T(T \rightarrow 0) \equiv \gamma$ of $\text{Eu}_{0.83}\text{Fe}_4\text{Sb}_{12}$ extrapolates to about 100 mJ/molK², isostructural $\text{La}_{0.83}\text{Fe}_4\text{Sb}_{12}$ exhibits a much larger value, 185 mJ/molK².

The phonon contribution to the specific heat is analyzed considering a Debye spectrum together with two Einstein modes, and additionally by a single Einstein contribution accounting for the behavior of the weakly bound rare-earth ion,

$$C_{ph}(T) = 12 \frac{3R}{\omega_D^3} \int_0^{\omega_D} \frac{\omega^2 \left(\frac{\omega}{2T}\right)^2}{\sinh^2\left(\frac{\omega}{2T}\right)} d\omega + \sum_{i=1,2} c_i R \frac{\left(\frac{\omega_{E_i}}{2T}\right)^2}{\sinh^2\left(\frac{\omega_{E_i}}{2T}\right)}. \quad (1)$$

Equation (1) was successfully applied to binary RhSb_3 and IrSb_3 (Ref. 10) considering three acoustic and nine optical branches of the phonon dispersion. For the polyanion $[\text{Fe}_4\text{Sb}_{12}]$ in the filled skutterudite $\text{La}_{0.83}\text{Fe}_4\text{Sb}_{12}$ the phonon modes are represented by $(12 \times)$ one Debye and two Einstein functions $(27 \times f_{E_1} + 9 \times f_{E_2})$. In order to account for La in the filled skutterudite, simply one further Einstein function has to be added to Eq. (1) to describe the increased number of phonon modes due to the additional $x = 0.83$ atoms per f.u. of $\text{La}_{0.83}\text{Fe}_4\text{Sb}_{12}$. The index of the second term of Eq. (1) is then $i = 1, 2, 3$ with $c_3 = 3 \times 0.83$. Using $c_1 = 27$ and $c_2 = 9$, a reasonable parametrization of $C_{ph}(T)$ is possible in a temperature range from 2–100 K (solid line, Fig. 3). The parameters obtained by least-squares fits are $\omega_D = 156$, $\omega_{E_1} = 270$, $\omega_{E_2} = 125$, and $\omega_{E_3} = 270$ K. The calculation of the low-temperature Debye temperature Θ_D^{LT} according to $\Theta_D^{LT} = \sqrt[3]{1944 \times (16 + 0.83)/\beta}$, where β is the slope of C/T vs T^2 at low temperatures yields $\Theta_D = 348$ K.

In general the magnetic contribution to the specific heat C_{mag} of magnetic compounds is obtained from the difference

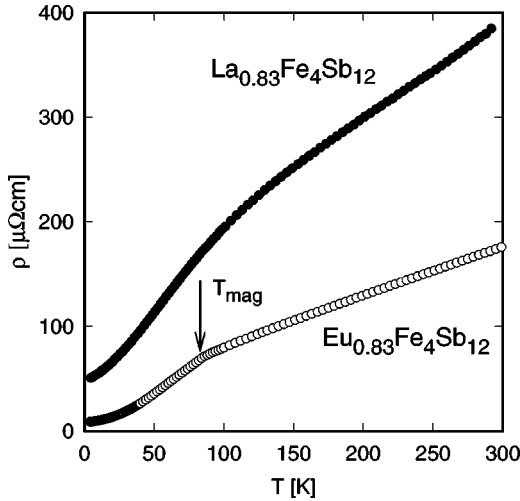


FIG. 4. Temperature-dependent electrical resistivity $\rho(T)$ of $\text{Eu}_{0.83}\text{Fe}_4\text{Sb}_{12}$ and $\text{La}_{0.83}\text{Fe}_4\text{Sb}_{12}$.

of the heat capacities of the magnetic and a nonmagnetic homologous isotypic compound. Among rare-earth systems, the most widely used nonmagnetic representatives are isostructural La compounds. Although many cases are known in which the phonon spectrum of La compounds differs significantly from that of isomorphous Y or Lu systems,¹⁶ we are constrained by the fact that skutterudites form only with the large rare-earth members, excluding Y and Lu homologs. Despite such shortcomings, we attempted at least to estimate the order of magnitude of C_{mag} of $\text{Eu}_{0.83}\text{Fe}_4\text{Sb}_{12}$ by comparison with $\text{La}_{0.83}\text{Fe}_4\text{Sb}_{12}$ ($\Delta C_p \approx C_{\text{mag}}$). Additionally, for both compounds the linear electronic contribution was subtracted, too. Plotted in Fig. 3 (right axis) is the magnetic entropy S_{mag} as derived from $\int C_{\text{mag}}/TdT$. S_{mag} continuously increases and a kink at T_{mag} reflects the ordering temperature. The release of entropy at this temperature is about 24 J/molK, larger than expected for Eu in a nearly 2+ state [i.e., $j = 7/2$, $S_{\text{theor}} = R \ln(2j+1) = 17.28$ J/molK]. The deduced significant surplus of entropy release can be attributed either to the mentioned differences in the phonon spectra or to subtle differences in the magnetic contribution of the $[\text{Fe}_4\text{Sb}_{12}]$ polyanions.

3. Transport properties and pressure effect

In order to evaluate the thermoelectric performance of $\text{Eu}_{0.83}\text{Fe}_4\text{Sb}_{12}$, we have measured various transport coefficients of this compound. Plotted in Fig. 4 is the temperature-dependent resistivity ρ of $\text{Eu}_{0.83}\text{Fe}_4\text{Sb}_{12}$ in comparison with that of $\text{La}_{0.83}\text{Fe}_4\text{Sb}_{12}$. The overall behavior of $\text{Eu}_{0.83}\text{Fe}_4\text{Sb}_{12}$ reflects a metallic state with absolute $\rho(T)$ values significantly lower than those of most of the known antimony-based skutterudites. The pronounced kink around 84 K is due to the onset of magnetic order. The linear dependency of $\rho(T)$ above the ordering temperature implies spin disorder scattering of the conduction electrons in the absence of pronounced crystal-field splitting, corroborating the essentially divalent electronic configuration of the Eu ions (the ground state then matches Gd with $^8S_{7/2}$).

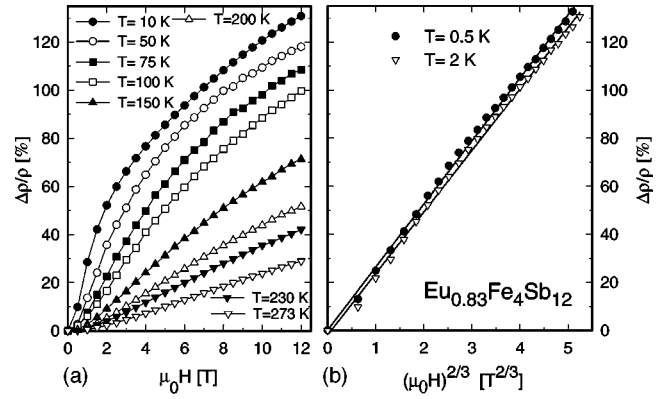


FIG. 5. (a) Isothermal magnetoresistance $\Delta\rho/\rho$ of $\text{Eu}_{0.83}\text{Fe}_4\text{Sb}_{12}$. (b) $\Delta\rho/\rho$ of $\text{Eu}_{0.83}\text{Fe}_4\text{Sb}_{12}$ vs $(\mu_0H)^{(2/3)}$.

Although $\text{La}_{0.83}\text{Fe}_4\text{Sb}_{12}$ is considered to be a nonmagnetic simple metallic compound, the strong curvature in $\rho(T)$ prevents a description in terms of the Bloch-Grüneisen law. Even the addition of the Mott-Jones term κT^3 , accounting for a narrow feature in the density of states near the Fermi energy, does not reveal a satisfying description. This most likely indicates additional magnetic interactions of the conduction electrons with the $[\text{Fe}_4\text{Sb}_{12}]$ polyanion complex.

The field response of the electrical resistivity of $\text{Eu}_{0.83}\text{Fe}_4\text{Sb}_{12}$ is presented in Figs. 5(a) and (b) revealing a positive magnetoresistance for the entire region measured (0–12 T and 0.5–300 K). The most interesting feature, however, is the enormous size of the magnetoresistance effect: for 12 T and $T = 1$ K, $\Delta\rho/\rho$ amounts to 130%, and even at room temperature $\Delta\rho/\rho$ is as large as 30%. At low temperatures, the field dependence of $\Delta\rho/\rho$ is found to behave proportional to $(\mu_0H)^{2/3}$ [compare Fig. 5(b)]. It is interesting to note that isostructural $\text{CeRu}_4\text{Sb}_{12}$ is also characterized by such unusual large values of the magnetoresistance for temperatures up to room temperature.¹⁷

A typical ferromagnet would exhibit, in general, a negative magnetoresistance.¹⁸ Thus, in combination with the non-linear reciprocal susceptibility of $\text{Eu}_{0.83}\text{Fe}_4\text{Sb}_{12}$, the observed positive magnetoresistance points either to a canted ferromagnet or a ferrimagnetic ground state. In such a case, sufficiently high external magnetic fields would cause a field-induced ferromagnetic alignment and above a certain critical field the magnetoresistance is expected to cross over to negative values. A corresponding high-field study is in progress. However, a behavior $\Delta\rho/\rho \propto (\mu_0H)^{2/3}$ over a significant field range and the large values, even in the paramagnetic temperature range, do not entirely exclude the classical magnetoresistance.¹⁹

As is already obvious from the isothermal field measurements, the field increase causes the resistivity to increase too, more than double its value at low temperatures [see Fig. 6(a)]. In order to analyze the temperature dependence of $\rho(T, H)$, least-squares fits according to $\rho = \rho_0 + AT^n$ were performed, leading to a value of n close to 2 for the whole field range. This is also seen from Fig. 6(b), where the data are plotted on a T^2 temperature scale. A T^2 behavior of the electrical resistivity well below the ordering temperature of

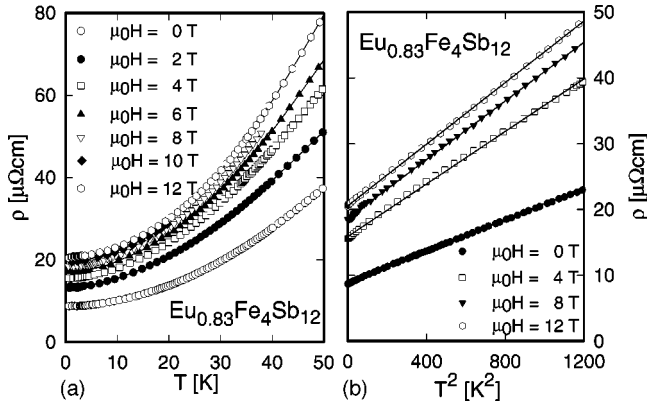


FIG. 6. (a) Temperature-dependent electrical resistivity $\rho(T)$ of $\text{Eu}_{0.83}\text{Fe}_4\text{Sb}_{12}$ for various values of external magnetic fields. (b) $\rho(T, H)$ of $\text{Eu}_{0.83}\text{Fe}_4\text{Sb}_{12}$ vs T^2 .

$\text{Eu}_{0.83}\text{Fe}_4\text{Sb}_{12}$ would be in line with ferromagnetic-like spin waves, thus not in contradiction to the supposed ground state of this compound.

The response of $\text{Eu}_{0.83}\text{Fe}_4\text{Sb}_{12}$ to pressure yields both a slight increase in the overall resistivity and an increase in the magnetic phase-transition temperature at a rate of about 0.5 K/kbar (see Fig. 7 and its inset). The positive change of dT_{mag}/dp can be considered as a hint to a localized moment behavior of the Eu ion. Pressure drives the magnetic ions closer together, thus Ruderman-Kittel-Kasuya-Yosida interactions enhance and so does the phase-transition temperature. Systems that are dominated by itinerant magnetic moments, on the contrary, are expected to exhibit the opposite pressure response.²⁰

The Grüneisen parameter related to the phase transition $\Gamma_{T_{\text{mag}}}$ follows from

$$\Gamma_{T_{\text{mag}}} = -\frac{\partial \ln T_{\text{mag}}}{\partial \ln V} = B_0 \frac{\partial \ln T_{\text{mag}}}{\partial p} = \frac{B_0}{T_{\text{mag}}} \frac{\partial T_{\text{mag}}}{\partial p}, \quad (2)$$

where B_0 is the bulk modulus of the system.²¹ With $T_{\text{mag}} = 84$ K, $\partial T_{\text{mag}}/\partial p = 0.5$ K/kbar and, as a first approximation,

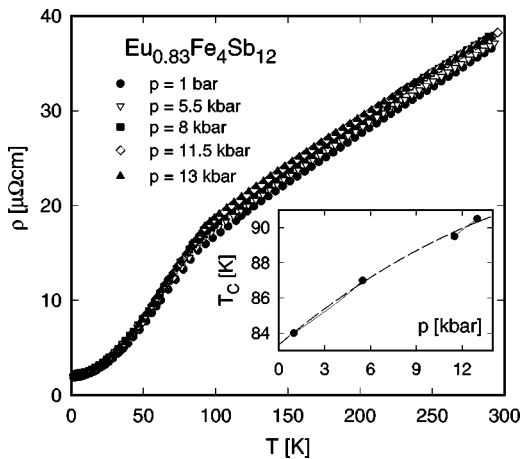


FIG. 7. Temperature- and pressure-dependent resistivity $\rho(T, p)$ of $\text{Eu}_{0.83}\text{Fe}_4\text{Sb}_{12}$. The inset shows the pressure response of the magnetic phase transition.

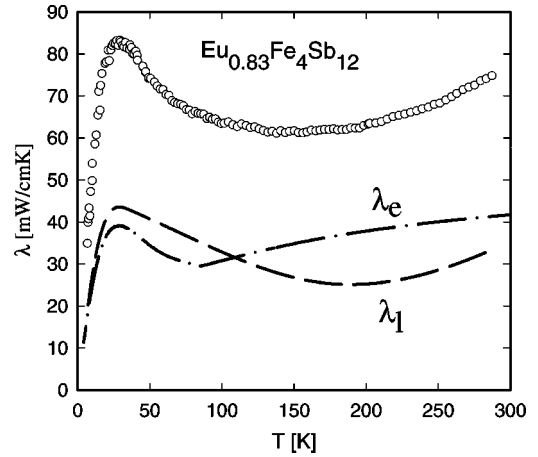


FIG. 8. Temperature-dependent thermal-conductivity data $\lambda(T)$ of $\text{Eu}_{0.83}\text{Fe}_4\text{Sb}_{12}$. The lattice λ_l and the electronic contribution λ_e to the thermal conductivity are shown as dashed and dash-dotted lines, respectively.

assuming $B_0 = 1000$ kbar, $\Gamma_{T_{\text{mag}}} \approx 6$. Such an order of magnitude can be considered as typical for stable magnetic systems, very frequently found in rare-earth intermetallic compounds.

Measurements of the thermal conductivity λ of $\text{Eu}_{0.83}\text{Fe}_4\text{Sb}_{12}$ are summarized in Fig. 8. In general, the observed thermal conductivity is small, but the overall value is substantially larger than values reported for several other filled skutterudites.²² This fact results from the extreme low resistivity of the compound, together with a large residual resistivity ratio value of about 15. Good electrical conductivity causes the electronic contribution to the total thermal conductivity to be a significant portion of the measured quantity.

The total thermal conductivity λ is usually given by $\lambda = \lambda_e + \lambda_l$ where λ_e represents the electronic part and λ_l the lattice contribution. In the case of simple metals, the Wiedemann-Franz law is expected to be valid, thus, $\lambda_e = L_0 T/\rho$. $L_0 = 2.45 \times 10^{-8}$ $\text{W}\Omega\text{K}^{-2}$ is the Lorenz number (derived in the scope of the free-electron model) and ρ is the electrical resistivity of the sample.

Applying the Wiedemann-Franz law to systems other than simple metals in order to separate λ_e and λ_l results in crude approximations only; nevertheless this law is widely used in the field of thermoelectric materials (compare Ref. 22) to define the lattice thermal conductivity. The latter contribution λ_l follows then simply from $\lambda_l = \lambda - L_0 T/\rho$. Results of such an analysis are shown in Fig. 8 as dashed and dash-dotted lines. Although this analysis should not be overstressed, one can conclude that λ_e is large, and even exceeds at elevated temperatures the lattice contribution to the total measured effect.

In Fig. 9, the thermoelectric power $S(T)$ is displayed for $\text{Eu}_{0.83}\text{Fe}_4\text{Sb}_{12}$ and $\text{La}_{0.83}\text{Fe}_4\text{Sb}_{12}$. In the magnetically ordered range, $S(T)$ is predominantly negative and small, however, the paramagnetic temperature range is characterized by an almost linear behavior, reaching about 50 $\mu\text{V}/\text{K}$ near 300 K. A kink in $S(T)$ in the proximity of 84 K traces also the phase-transition temperature. For the purpose of comparison,

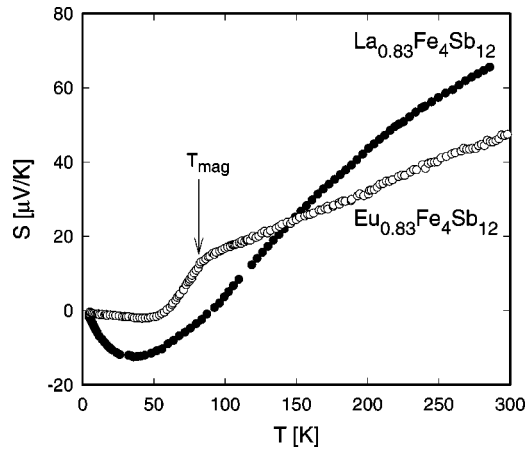


FIG. 9. Temperature-dependent Seebeck coefficient $S(T)$ of $\text{Eu}_{0.83}\text{Fe}_4\text{Sb}_{12}$ and $\text{La}_{0.83}\text{Fe}_4\text{Sb}_{12}$.

$S(T)$ of the isomorphous compound $\text{La}_{0.83}\text{Fe}_4\text{Sb}_{12}$ is added. Besides a smooth minimum with negative values, $S(T)$ of the latter grows continuously up to about $70 \mu\text{V/K}$. Well above the magnetic ordering temperature of the Eu compound, $S(T)$ of $\text{La}_{0.83}\text{Fe}_4\text{Sb}_{12}$ is much larger than $S(T)$ of $\text{Eu}_{0.83}\text{Fe}_4\text{Sb}_{12}$. In terms of a simple count of carriers, $[\text{Fe}_4\text{Sb}_{12}]$ exhibits four holes. The filling of the binary skutterudite—which, in the mentioned case, is not stable—by electropositive elements like La or Eu then compensates partially the holes and thus reduces the number of carriers. Since Eu exhibits an almost $2+$ state $4f^7$ electronic configuration), less holes are compensated by electrons in comparison to the case of $\text{La}_{0.83}\text{Fe}_4\text{Sb}_{12}$. Hence, the lower number of carriers in $\text{La}_{0.83}\text{Fe}_4\text{Sb}_{12}$ causes the experimentally observed larger thermopower values and the positive sign matches with a holelike transport.

IV. CONCLUSION

The study of bulk properties performed on $\text{Eu}_{0.83}\text{Fe}_4\text{Sb}_{12}$ revealed magnetic ordering below 84 K. The appearance of a spontaneous magnetization excludes then an antiferromagnetic ground state.

Transport processes observed in $\text{Eu}_{0.83}\text{Fe}_4\text{Sb}_{12}$ as well as in $\text{La}_{0.83}\text{Fe}_4\text{Sb}_{12}$ are dominated by p type conductivity. This is understood from just a partial compensation of the electron deficient $[\text{Fe}_4\text{Sb}_{12}]$ polyanion by the electropositive elements, i.e., Eu and La. A recently performed Hall measurement²³ at room temperature allowed us to estimate the carrier concentration of $\text{Eu}_{0.83}\text{Fe}_4\text{Sb}_{12}$, which was 2.1 holes per formula unit. This is in excellent agreement with a

simple carrier count assuming an almost $2+$ state of the Eu ion. This number evidences a high carrier concentration, thus the Seebeck coefficient is restricted while both the electrical as well as the thermal conductivity should be large. In fact, these predictions are verified from the experimental results. The comparison of $\text{Eu}_{0.83}\text{Fe}_4\text{Sb}_{12}$ with isomorphous $\text{La}_{0.83}\text{Fe}_4\text{Sb}_{12}$, where scattering processes on the rare-earth magnetic moments are absent, shows that the number of free carriers is the essential parameter in these compounds. Since La, in general, exhibits the $3+$ state, the compensation of the electron deficient $[\text{Fe}_4\text{Sb}_{12}]$ is much more efficient than with divalent Eu. Thus, the carrier concentration is much more decreased and consequently, the Seebeck coefficient becomes larger. Even quantities like $\rho(T)$ and $\lambda(T)$ seem to be influenced by the change in the hole concentration when proceeding from $\text{Eu}_{0.83}\text{Fe}_4\text{Sb}_{12}$ to $\text{La}_{0.83}\text{Fe}_4\text{Sb}_{12}$ as derived from a significantly larger resistivity, while the thermal conductivity of La-based skutterudites²² has a room-temperature value of roughly 15 mW/cmK , i.e., about four times smaller than that of $\text{Eu}_{0.83}\text{Fe}_4\text{Sb}_{12}$.

In order to significantly enhance the figure of merit Z of this Eu-based skutterudite ($ZT \approx 0.08$ at room temperature), the number of carriers has to be reduced. This can be done by a substitution of Fe/Co. In fact, preliminary measurements on $\text{Eu}_y(\text{Fe}_{4-x}\text{Co}_x)\text{Sb}_{12}$ show that a lowering of the carrier number by increasing the Co content doubles the Seebeck coefficient at room temperature, and moreover, the system crosses over to electron-type transport beyond a critical Co concentration ($x > 3$).²⁴

The observation of an unexpected large magnetoresistance over the entire temperature range covered is the most outstanding property observed. The physical origin of this behavior is yet unknown. However, a sample with a canted magnetic structure (possessing a net magnetization) can increase its resistivity values when the field strength rises owing to a rotation of the moments. Once the field-induced order becomes perfect, the magnetoresistance should decrease. Such an explanation, of course, does not hold for the paramagnetic temperature range.

ACKNOWLEDGMENTS

This research was supported by the Austrian FWF under Grant Nos. P13778-PHY and P12899-PHY as well as by a grant for an international joint research project NEDO (Japan). The authors gratefully acknowledge the support of the Austrian-Polish Scientific-Technical Exchange Program (OEAD, project 13/99). A.G. is grateful to the Romanian ANSTI, Grant No. 6121.

*On leave from the National Institute of Material Physics, P.O. Box MG-07, 76900 Bucharest-Magurele, Romania.

†On leave from the Dipartimento di Fisica “A. Volta,” Università degli studi di Pavia, I-27100 Pavia.

‡On leave from the W. Trzebiatowski Institute for Low Temperature and Structure Research, Polish Academy of Sciences, P.O. Box 1410, P-50-950 Wrocław, Poland.

¹G.S. Nolas, D.T. Morelli, and T.M. Tritt, *Annu. Rev. Mater. Sci.* **29**, 89 (1999), and references therein.

²M.S. Torikachvili, J.W. Chen, Y. Dalichaouch, R.P. Guertin, M.W. McElfresh, C. Rossel, M.B. Maple, and G.P. Meisner, *Phys. Rev. B* **36**, 8660 (1987).

³I. Shirovani, T. Adachi, K. Tachi, S. Todo, K. Nozawa, T. Yagi, and M. Kinoshita, *J. Phys. Chem. Solids* **57**, 211 (1996).

- ⁴I. Shirovani, T. Uchiumi, K. Ohno, C. Sekine, Y. Nakazawa, K. Kanoda, S. Todo, and T. Yagi, *Phys. Rev. B* **56**, 7866 (1997).
- ⁵C. Sekine, T. Uchiumi, I. Shirovani, and T. Yagi, *Phys. Rev. Lett.* **79**, 3218 (1997).
- ⁶M.E. Danebrock, C.B.H. Evers, and W. Jeitschko, *J. Phys. Chem. Solids* **57**, 381 (1996).
- ⁷D.T. Morelli and G.P. Meisner, *J. Appl. Phys.* **77**, 3777 (1995).
- ⁸D.A. Gajewski, M.R. Dilley, E.D. Bauer, E.J. Freeman, R. Chau, M.B. Maple, D. Mandrus, B.C. Sales, and A.H. Lacerda, *J. Phys.: Condens. Matter* **10**, 6973 (1998).
- ⁹N.R. Dilley, E.J. Freeman, E.D. Bauer, and M.B. Maple, *Phys. Rev. B* **58**, 6287 (1998).
- ¹⁰E. Bauer, A. Galatanu, H. Michor, G. Hilscher, P. Rogl, P. Boulet, and H. Noël, *Eur. Phys. J. B* **14**, 483 (2000).
- ¹¹W. Wacha, Diploma thesis, Technische Universität Wien, 1989.
- ¹²A. Leithe-Jasper, D. Kaczorowski, P. Rogl, J. Bogner, M. Reissner, W. Steiner, G. Wiesinger, and C. Godart, *Solid State Commun.* **109**, 395 (1999).
- ¹³J. Rodriguez-Carvajal, FULLPROF: A Program for Rietveld Refinement and Pattern Matching Analysis, Abstracts of the Satellite Meeting on Powder Diffraction of the XV Congress of the International Union of Crystallography, Toulouse, France, 1990, p. 127.
- ¹⁴A. Eiling and J. Schilling, *J. Phys. F: Met. Phys.* **11**, 623 (1981).
- ¹⁵W. Jeitschko and D.J. Braun, *Acta Crystallogr., Sect. B: Struct. Crystallogr. Cryst. Chem.* **B33**, 3401 (1977).
- ¹⁶C.T. Yeh, W. Reichardt, B. Renker, N. Nücker, and M. Loewenhaupt, *J. Phys. Colloq.* **C6**, 371 (1981).
- ¹⁷E.D. Bauer and B. Maple (private communication).
- ¹⁸H. Yamada and S. Takada, *J. Phys. Soc. Jpn.* **34**, 51 (1973).
- ¹⁹E. Gratz, in *The Encyclopedia of Materials*, edited by K.H.J. Buschow (Pergamon, New York, 2001).
- ²⁰T.F. Smith, J.A. Mydosh, and E.P. Wolfarth, *Phys. Rev. Lett.* **27**, 1732 (1971).
- ²¹J.D. Thompson, in *Frontiers in Solid State Sciences*, edited by L.C. Gupta and M.S. Multani (World Scientific, Singapore, 1993), Vol. 2, p. 107.
- ²²B.C. Sales, D. Mandrus, B.C. Chakoumakos, V. Keppens, and J.R. Thompson, *Phys. Rev. B* **56**, 15 081 (1997).
- ²³V.L. Kuznetsov and D.M. Rowe, *J. Phys.: Condens. Matter* **12**, 7915 (2000).
- ²⁴St. Berger (unpublished).